

BCS-BEC crossover in quantum confined superconductors

Andrea Guidini · Luca Flammia · Milorad V. Milošević · Andrea Perali

Received: date / Accepted: date

Abstract Ultranarrow superconductors are in the strong quantum confinement regime with formation of multiple coherent condensates associated with the many subbands of the electronic structure. Here we analyze the multiband BCS-BEC crossover induced by the chemical potential tuned close to a subband bottom, in correspondence of a superconducting shape resonance. The evolution of the condensate fraction and of the pair correlation length in the ground state as functions of the chemical potential demonstrates the tunability of the BCS-BEC crossover for the condensate component of the selected subband. The extension of the crossover regime increases when the pairing strength and/or the characteristic energy of the interaction get larger. Our results indicate the coexistence of large and small Cooper pairs in the crossover regime, leading to the optimal parameter configuration for high transition temperature superconductivity.

Keywords BCS-BEC crossover · Shape resonant superconductivity · Ultrathin superconductors · Superstripes

Andrea Guidini
School of Science and Technology, Physics Division, University of Camerino, 62032 Camerino, Italy
E-mail: andrea.guidini@unicam.it

Luca Flammia
School of Science and Technology, Physics Division, University of Camerino, 62032 Camerino, Italy
Departement Fysica, Universiteit Antwerpen, Groenenborgerlaan 171, B-2020 Antwerpen, Belgium

Milorad V. Milošević
Departement Fysica, Universiteit Antwerpen, Groenenborgerlaan 171, B-2020 Antwerpen, Belgium

Andrea Perali
School of Pharmacy, Physics Unit, University of Camerino, 62032 Camerino, Italy

PACS 74.20.-z · 74.20.Fg · 74.25.Dw

1 Introduction

Control and enhancement of superconductivity when the material geometry is reduced at the nano or atomic scale has been predicted long time ago. First systems considered have been ultrathin superconducting slabs of metals [1] and superconducting stripes [2], with the further extension to the superlattice of stripes, where the spatial repetition of the stripes can stabilize macroscopic superconductivity against low dimensional fluctuations of the order parameter [3]. Quantum size oscillations, shape resonances, and sizable amplification of the superconducting critical temperature have been experimentally confirmed and theoretically analyzed in metallic aluminum and tin nanowires of cylindrical shape [4]. Interestingly, the Authors of Ref.[5] predicted a strong renormalization of the chemical potential and the possibility of the complete condensation of all the electrons of the subband in which the chemical potential is close to its energy bottom, giving rise to the coexistence of BCS-like and BEC-like pairs. A more detailed study of the BCS-BEC crossover in superconducting nanofilms induced by the quantum confinement has been recently conducted in Ref.[6].

In another class of systems, ultracold cigar-shaped fermions, the quantum confinement induces the formation of a series of multiple subbands. In Ref.[7] it has been found that in the superfluid state of these systems the overall condensate is a coherent mixture of partial subband condensates. Each partial condensate undergoes a BCS-BEC crossover when the chemical potential is tuned at the energy bottom of the corresponding subband.

More recently, the discovery of the MgB₂ superconductor and of the different families of iron-based superconductors definitely opened a new field of investigation in condensed matter physics: the multicomponent (or multigap / multiband) superconductivity [8] (see also the web portal of the International Network on Multi-component Superconductivity and Superfluidity: <http://www.multisuper.org>). For iron-based superconductors the central role played by one of the bands being in the BCS-BEC crossover was predicted in Ref.[9]. Moreover, the presence of one band in the BCS-BEC crossover was predicted to be a key feature for diverse high temperature superconductors in Ref.[10]. Recently, evidences of the BCS-BEC crossover in the small pockets of the Fermi surface of multi-band superconductors have been reported. ARPES in iron-calchogenide superconductors has reported a value of the ratio between the superconducting gap to the Fermi energy of order one in the shallow upper bands [11,12]. This phenomenology is now accepted to be a generic important feature of all iron-based superconductors, as discussed in Ref.[13]. The observed phenomenology is the same as in ultracold fermions [14,15,16]. A detailed discussion on these observations pointing to a component selective BCS-BEC crossover in iron-based superconductors and in related systems have been reported in [17]. This is the optimal configuration for (very) high-T_c superconductivity. Multi-band BCS-BEC crossover makes possible the screening of superconducting fluctuations, as shown in a two-band superconductor by a Ginzburg-Landau approach, see Ref.[18]. In addition, multi-band BCS-BEC crossover is expected to induce an important discrepancy of length scales of the different superconducting condensates when the chemical potential approaches a band bottom of the multi-band system. In this shape-resonant configuration, interesting vortex phenomena with possible fractional states [19], non-monotonic vortex interaction [20], and hidden criticality [21] are predicted and could be experimentally observed.

Here we report on a simple physical realization of the multiband BCS-BEC crossover induced by the quantum confinement in superconducting slabs at the atomic limit. To capture the relevant and essential physics, we limit our analysis to the first two subbands generated by the quantum confinement. We consider an effective s-wave attractive interaction with an energy cutoff, including the important subband dependence induced by the reconfiguration of the pairing at the atomic scale. By evaluating the superconducting ground state properties at a mean-field level of approximation, we obtain the selective BCS-BEC crossover when the chemical potential is tuned close to the second subband bottom. The characterization of this crossover is obtained by

evaluating the zero temperature condensate fraction of the partial condensate of the second subband and the correlation length of Cooper pairs forming in the same subband.

2 Model and methods

We consider a two dimensional two-band system of interacting fermions at $T = 0$. The equations and relative discussions for band dispersion, gap, density, condensate fraction and pair correlation length are the same as discussed in Ref.[17]. We here recall only the equations and the most important remarks.

The electronic subbands have a parabolic dispersion of the form

$$\xi_i(\mathbf{k}) = \frac{\mathbf{k}^2}{2m} - \mu + \varepsilon_i, \quad (1)$$

where m is the effective mass, which is taken equal in the two subbands, μ is the chemical potential and ε_i are the energies of the subband bottoms. The index $i=1, 2$ labels the subbands: 1 stands for the lower subband while 2 for the upper. Here ε_1 is set to zero. The sketch of the subbands and of the corresponding Fermi surfaces can be seen in Fig. 1 of Ref.[17], with the difference that for the present work the picture presents the two-dimensional Fermi surfaces.

The effective pairing attraction is taken in a separable form and with an energy cutoff ω_0 . In contrast with Ref.[17], here the pairing interaction does not change structure when the chemical potential crosses the bottom of one of the subbands. Moreover, because the motion along the z -axis is tightly bound, the bare strengths of the potential that control the intraband and the interband Josephson-like pairing between the two bands are related by $V_{ij}^0 = V^0(1 + \frac{1}{2}\delta_{ij})$. The pairing potential can be then written as

$$V_{ij}(\mathbf{k}, \mathbf{k}') = -V^0(1 + \frac{1}{2}\delta_{ij}) \Theta(\omega_0 - |\xi_i(\mathbf{k})|) \times \Theta(\omega_0 - |\xi_j(\mathbf{k}')|), \quad (2)$$

where V^0 is the (positive) strength of the attractive (s-wave) potential.

The \mathbf{k} -dependence of the gaps is given by

$$\Delta_i(\mathbf{k}) = \Delta_i \Theta(\omega_0 - |\xi_i(\mathbf{k})|). \quad (3)$$

The coupled mean-field equations for the gaps are

$$\Delta_1(\mathbf{k}) = -\frac{1}{\Omega} \sum_{\mathbf{k}'} \left[V_{11}(\mathbf{k}, \mathbf{k}') \frac{\Delta_1(\mathbf{k}')}{2\sqrt{\xi_1(\mathbf{k}')^2 + \Delta_1(\mathbf{k}')^2}} + V_{12}(\mathbf{k}, \mathbf{k}') \frac{\Delta_2(\mathbf{k}')}{2\sqrt{\xi_2(\mathbf{k}')^2 + \Delta_2(\mathbf{k}')^2}} \right], \quad (4)$$

$$\Delta_2(\mathbf{k}) = -\frac{1}{\Omega} \sum_{\mathbf{k}'} \left[V_{21}(\mathbf{k}, \mathbf{k}') \frac{\Delta_1(\mathbf{k}')}{2\sqrt{\xi_1(\mathbf{k}')^2 + \Delta_1(\mathbf{k}')^2}} + V_{22}(\mathbf{k}, \mathbf{k}') \frac{\Delta_2(\mathbf{k}')}{2\sqrt{\xi_2(\mathbf{k}')^2 + \Delta_2(\mathbf{k}')^2}} \right], \quad (5)$$

being Ω the area occupied by the system.

In this work the density is not fixed and it is given by

$$n_i = \frac{2}{\Omega} \sum_{\mathbf{k}} v_i(\mathbf{k})^2, \quad (6)$$

where $v_i(\mathbf{k})$ is the BCS weight of the occupied states

$$v_i(\mathbf{k})^2 = \frac{1}{2} \left[1 - \frac{\xi_i(\mathbf{k})}{\sqrt{\xi_i(\mathbf{k})^2 + \Delta_i(\mathbf{k})^2}} \right]. \quad (7)$$

The condensate fraction α_i and pair correlation length ξ_i are given by

$$\alpha_i = \frac{\sum_{\mathbf{k}} (u_i(\mathbf{k})v_i(\mathbf{k}))^2}{\sum_{\mathbf{k}} v_i(\mathbf{k})^2}, \quad (8)$$

$$\xi_i = \left[\frac{\sum_{\mathbf{k}} |\nabla_{\mathbf{k}} (u_i(\mathbf{k})v_i(\mathbf{k}))|^2}{\sum_{\mathbf{k}} (u_i(\mathbf{k})v_i(\mathbf{k}))^2} \right]^{\frac{1}{2}} \quad (9)$$

where $u_i(\mathbf{k})^2 = 1 - v_i(\mathbf{k})^2$.

The sums over \mathbf{k} are replaced by two-dimensional integrals over momenta and then by integrals over the energy variable, after introducing the 2D density of states $N_{2D} = m/(2\pi)$.

The integrals of Eqs. (4-6) and (8) can be expressed in a closed form, while Eq. (9) is calculated numerically. Indeed, to obtain the pair correlation length we introduce a smooth function in place of the step function associated to the \mathbf{k} -dependent gap of Eq. (3) in order to obtain well defined partial derivatives, and then we calculate numerically the integrals.

3 Results

We present here the plots of superconducting gaps, condensate fractions and pair correlation lengths as functions of the ratio $(\mu - \varepsilon_2)/\omega_0$, which is the Lifshitz parameter measuring the distance from the Lifshitz transition in units of the energy cutoff of the pairing interactions ω_0 , for a given value of the cutoff energy $\omega_0/\varepsilon_2 = 0.5$ and for two couplings $\lambda \equiv N_{2D}V^0 = 0.2$ and 0.3 . Gaps are units of ω_0 as well as in units of the Fermi energies of the bands $E_{F_i} = \frac{2\pi}{m}n_i$ where n_i is calculated by Eq. (6). The pair correlation lengths are measured in units of $1/k_{F_i} = 1/\sqrt{4\pi n_i}$.

In Fig. 1 we present the superconducting gaps $\Delta_{1,2}$ in units of ω_0 as functions of the chemical potential μ in units of ω_0 and referred to the bottom of the second

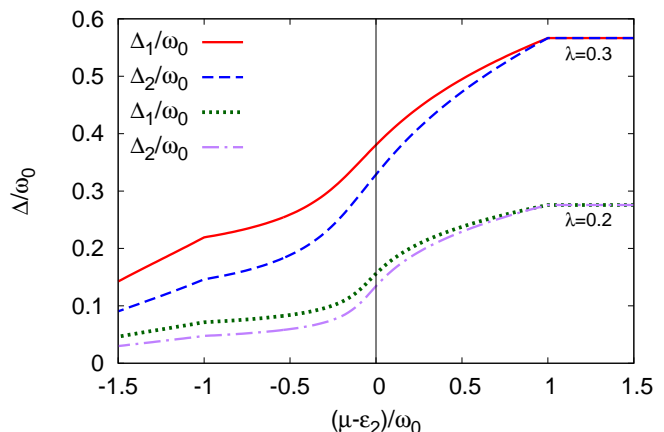


Fig. 1 Superconducting gaps $\Delta_{1,2}$ in units of ω_0 as functions of the chemical potential μ in units of ω_0 and referred to the bottom of the second subband ε_2 for $\omega_0/\varepsilon_2=0.5$ and two values of coupling $\lambda=0.3, 0.2$.

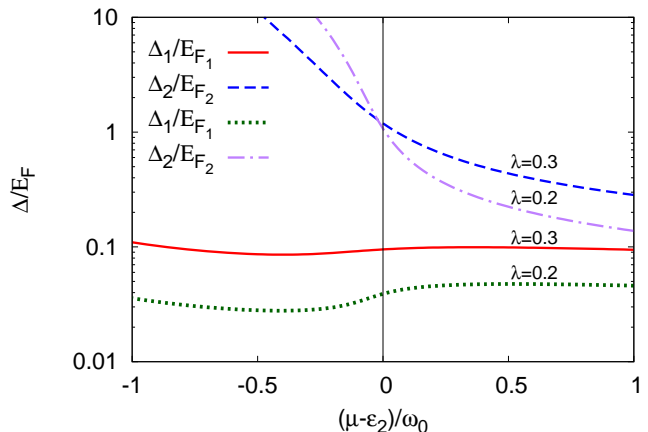


Fig. 2 Superconducting gaps $\Delta_{1,2}$ in units of the Fermi energies $E_{F_{1,2}}$ as functions of the chemical potential μ in units of ω_0 and referred to the bottom of the second subband ε_2 for $\omega_0/\varepsilon_2=0.5$ and two values of coupling $\lambda=0.3, 0.2$.

subband ε_2 . The curves become flat when $\mu - \varepsilon_2 - \omega_0 \geq 0$.

In Fig. 2 we present the gaps in units of the Fermi energies of the subbands. The upper subband enters the BEC regime of pairing ($\Delta_2/E_{F_2} > 1$) when the chemical potential crosses the bottom of the subband. In particular when $\mu \sim \varepsilon_2$ one has $\Delta_2 \sim E_{F_2}$. The gap of the lower subband is instead less sensitive to μ and it signals that the pairing involving the lower subband is in the BCS regime.

In Fig. 3 we present the pair correlation lengths in units of the inverse of the Fermi wave-vectors of the bands. The evolution of the pair correlation length to describe the BCS-BEC crossover has been introduced in Ref. [22]. The lower subband is in the BCS regime

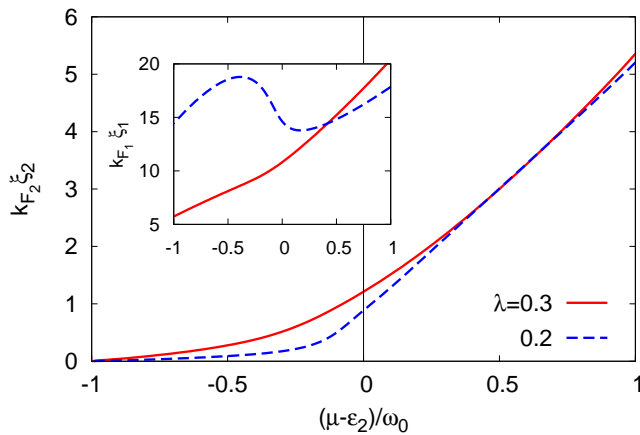


Fig. 3 Pair correlation lengths $\xi_{1,2}$ in units of $k_{F_{1,2}}^{-1}$ as functions of the chemical potential μ in units of ω_0 and referred to the bottom of the second subband ε_2 for $\omega_0/\varepsilon_2=0.5$ and two values of coupling $\lambda=0.3, 0.2$.

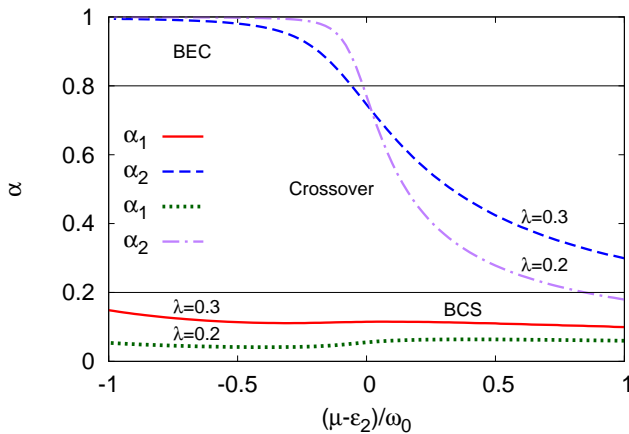


Fig. 4 Condensate fractions $\alpha_{1,2}$ as functions of the chemical potential μ in units of ω_0 and referred to the bottom of the second subband ε_2 for $\omega_0/\varepsilon_2=0.5$ and two values of coupling $\lambda=0.3, 0.2$. The boundaries of the BCS-BEC crossover are indicated with horizontal lines.

($k_F\xi \gg 1$), whereas the upper subband enters the BEC regime ($k_F\xi < 1$) when the chemical potential crosses ε_2 . It is interesting also to note the feedback of ξ_2 on ξ_1 when $\mu = \varepsilon_2$ for $\lambda = 0.2$. We found that this effect is more pronounced for small values of λ and ω_0 .

In Fig. 4 we present the partial condensate fractions $\alpha_{1,2}$. Here we fix the boundaries of the different pairing regimes according to Ref.[17]. The lower subband ($i = 1$) is in the BCS regime of pairing having a condensate fraction smaller than 0.2 ($\alpha_1 < 0.2$) for every value of the chemical potential. The upper subband ($i = 2$) is in the BEC regime, characterized by a partial condensate fraction larger than 0.8 ($0.8 < \alpha_2 < 1.0$), for $(\mu - \varepsilon_2)/\omega_0 < 0$ and in the crossover regime of the BCS-

BEC crossover ($0.2 < \alpha_2 < 0.8$) for $0 < (\mu - \varepsilon_2)/\omega_0 < 1$. Larger values of the chemical potential ($(\mu - \varepsilon_2)/\omega_0 > 1$) will drive the system to a partial condensate fraction lower than 0.2 also in the upper subband ($\alpha_2 < 0.2$). In this situation both the partial condensates of the two subbands are in the weakly-coupled BCS regime.

4 Conclusions

Quantum confinement of superconductors at the atomic scale can generate a coherent overlap of partial superconducting condensates which are in different regimes of the BCS-BEC crossover. We found that the ratio between the energy gap in one of the subbands and the local Fermi energy is the relevant experimental parameter to locate the partial condensate in the BCS-BEC crossover. Considering the second subband, when the chemical potential approaches the subband bottom the ratio Δ_2/E_{F_2} becomes of order 1 and the system enters the shape-resonant crossover regime when $0.3 < \Delta_2/E_{F_2} < 1.0$, with a rapid onset of the BEC regime for negative chemical potential with respect to the subband bottom, corresponding to $\Delta_2/E_{F_2} > 1.0$.

Acknowledgements We acknowledge A. Bianconi and A.A. Shanenko for useful discussions. A.P. acknowledges financial support from the University of Camerino under the project FAR “Control and enhancement of superconductivity by engineering materials at the nanoscale”. M.V.M. acknowledges support from the Research Foundation - Flanders (FWO) and the Special Research Funds of the University of Antwerp (BOF-UA). A.P. and M.V.M. acknowledge the collaboration within the MultiSuper International Network (<http://www.multisuper.org>) for exchange of ideas and suggestions.

References

1. Blatt, J.M.: Theory of Superconductivity, Academic Press, New York (1964)
2. Perali, A., Bianconi, A., Lanzara, A., Saini, N.L.: The gap amplification at a shape resonance in a superlattice of quantum stripes: a mechanism for high Tc. Solid State Commun. 100, 181-186 (1996)
3. Bianconi, A., Valletta, A., Perali, A., Saini, N.L.: High Tc superconductivity in a superlattice of quantum stripes. Solid State Commun. 102, 369-374 (1997)
4. Shanenko, A.A., Croitoru, M.D., Zgirski, M., Peeters, F.M., Arutyunov, K.: Size-dependent enhancement of superconductivity in nanowires. Phys. Rev. B 74, 052502 (4pp) (2006) and references therein
5. Bianconi, A., Valletta, A., Perali, A., Saini, N.L.: Superconductivity of a striped phase at the atomic limit. Physica C 296, 269-280 (1998)
6. Chen, Y.J., Shanenko, A.A., Perali, A., Peeters, F.M.: Superconducting nanofilms: molecule-like pairing induced by quantum confinement. Journal of Phys.:Condens. Matter 24, 185701 (8pp) (2012)

7. Shanenko, A.A., Croitoru, M.D., Vagov, A.V., Axt, V.M., Perali, A., Peeters, F.M.: Atypical BCS-BEC crossover induced by quantum-size effects. *Phys. Rev. A* 86, 033612 (7pp) (2012)
8. Milosevic, M.V., Perali, A.: Emergent phenomena in multicomponent superconductivity: an introduction to the focus issue. *Supercond. Sci. Technol.* 28, 060201 (4pp) (2015) and references therein
9. Caivano, R., Fratini, M., Poccia, N., Ricci, A., Puri, A., Ren, Z.-A., Dong, X.-L., Yang, J., Lu, W., Zhao, Z.-X., Barba, L., Bianconi, A.: Feshbach resonance and mesoscopic phase separation near a quantum critical point in multiband FeAs-based superconductors. *Supercond. Sci. Technol.* 22, 014004 (12pp) (2009)
10. Bianconi, A.: Feshbach shape resonance in multiband superconductivity in heterostructures. *Journal of Superconductivity* 18, 625-636 (2005)
11. Lubashevsky, Y., Lahoud, E., Chashka, K., Podolsky, D., Kanigel, A.: Shallow pockets and very strong coupling superconductivity in $\text{FeSe}_x\text{Te}_{1-x}$. *Nature Phys.* 8, 309-312 (2012)
12. Kasahara, S., Watashige, T., Hanaguri, T., Kohsaka, Y., Yamashita, T., Shimoyama, Y., Mizukami, Y., Endo, R., Ikeda, H., Aoyama, K., Terashima, T., Uji, S., Wolf, T., Löhneysen, H.v., Shibauchi, T., Matsuda, Y.: Field-induced superconducting phase of FeSe in the BCS-BEC cross-over. *PNAS* 111, 16309-16313 (2014).
13. Bianconi, A.: Quantum materials: shape resonances in superstripes. *Nature Phys.* 9, 536-537 (2013)
14. Perali, A., Palestini, F., Pieri, P., Strinati, G.C., Stewart, J.T., Gaebler, J.P., Drake, T.E., Jin, D.S.: Evolution of the normal state of a strongly interacting Fermi gas from a pseudogap phase to a molecular Bose gas. *Phys. Rev. Lett.* 106, 060402 (4pp) (2011)
15. Pieri, P., Perali, A., Strinati, G.C., Riedl, S., Wright, M.J., Altmeyer, A., Kohstall, C., Sánchez Guajardo, E.R., Hecker Denschlag, J., Grimm, R.: Pairing-gap, pseudo-gap, and no-gap phases in the radio-frequency spectra of a trapped unitary ^6Li gas. *Phys. Rev. A* 84, 011608(R) (4pp) (2011)
16. Palestini, F., Perali, A., Pieri, P., Strinati, G.C.: Dispersions, weights, and widths of the single-particle spectral function in the normal phase of a Fermi gas. *Phys. Rev. B* 85, 024517 (17pp) (2012)
17. Guidini, A., Perali, A.: Band-edge BCS-BEC crossover in a two-band superconductor: physical properties and detection parameters. *Supercond. Sci. Technol.* 27, 124002 (10pp) (2014)
18. Perali, A., Castellani, C., Di Castro, C., Grilli, M., Piegari, E., Varlamov, A.A.: Two-gap model for underdoped cuprate superconductors. *Phys. Rev. B* 62, R9295(R) (4pp) (2000)
19. Geurts, R., Milosevic, M.V., Peeters, F.M.: Vortex matter in mesoscopic two-gap superconducting disks: Influence of Josephson and magnetic coupling. *Phys. Rev. B* 81, 214514 (15pp) (2010)
20. Chaves, A., Komendová, L., Milosevic, M.V., Andrade Jr., J.S., Farias, G.A., Peeters, F.M.: Conditions for non-monotonic vortex interaction in two-band superconductors. *Phys. Rev. B* 83, 214523 (6pp) (2011)
21. Komendová, L., Chen, Y., Shanenko, A.A., Milosevic, M.V., Peeters, F.M.: Two-Band Superconductors: Hidden Criticality Deep in the Superconducting State. *Phys. Rev. Lett.* 108, 207002 (5pp) (2012)
22. Pistolesi, F., Strinati, G.C.: Evolution from BCS superconductivity to Bose condensation: role of the parameter $k_F\xi$. *Phys. Rev. B* 49, 6356 (4pp) (1994)